PAPER

Check for updates

Condensed dewdrops self-ejecting on sprayable superhydrophobic CNT/SiO₂ composite coating†

Shanlin Wang, Jing Zhang, Xinquan Yu and Youfa Zhang [iD] *

We report a type of novel condensed dewdrops self-ejecting coating from sprayable paint, which was prepared by a self-assembly process of SiO₂ nano-particles on hydroxylated carbon nano-tubes with subsequent chemical modification. This work enlarges the application of sprayable superhydrophobic coatings for the enhancement of condensation heat transfer.

It is indispensable to reduce the formation and accumulation of dew on the solid–gas interface in a cold and humid environment to increase condensation heat transfer.[1–3] Therefore, the suppression and desorption of dewing play an important role in maintaining the surface as dry as possible.[4,5] Based on this, superhydrophobic surfaces display great potential to improve heat transfer due to their remarkable abilities in reducing the departure size of condensate drops from the millimeter scale down to the micrometer scale and increasing the renewal frequency of condensate microdrops.[6,7] However, the superhydrophobicity with the Cassie state cannot always be present during condensation.[8] Beyond that, it is still challenging to eliminate the accumulation of dew in time and effectively. To solve this issue, nano-array and nano-porous structures have often been used to design condensed dewdrops self-ejecting (CDSE) surfaces.[9–17] Evidence from the literature[18,19] suggests that CDSE behaviors were triggered because the adhesion force is lower than the kinetic energy which was transferred from the gain in surface energy when two or more micro-drops coalesce. However, few references can be found about a sprayable superhydrophobic coating with CDSE effects, although it performs with attractive designability and cooperativity on various substrates.[20–22] Recently, sprayable superhydrophobic coatings have mainly been developed to achieve anti-fouling,[23] self-cleaning,[24] and anti-corrosion[25] functions. To realize the application of superhydrophobic coatings in the real world, their mechanical stability was usually strengthened by a suitable adhesive.[26]

As we know, carbon nano-tubes (CNT) have also been considered for creating superhydrophobic films due to their remarkable thermal and electrical conductivity.[27,28] However, only CNT nano-arrays, grown by chemical vapor deposition (CVD) methods, have been reported to present a CDSE

Jiangsu Key Laboratory of Advanced Metallic Materials, School of Materials Science and Engineering, Southeast University, Nanjing 211189, P. R. China. E-mail: yfzhang@seu.edu.cn

† Electronic supplementary information (ESI) available. See DOI: 10.1039/c7ra04102k

function.[29] That is to say, it must be an important technical improvement if we can obtain CDSE coating by spray-coating CNT paint. Inspired by two-tier composite structures,[30–32] we propose that sprayable CDSE coatings may be formed using nano-porous structures assembled from rough CNT.

In this communication, to achieve sprayable CDSE coatings, we designed a self-assembly process for the growth of SiO₂ nano-particles (SNP) on a hydroxylated CNT (HCNT) in an alkaline solution (pH ∼ 10.5). And then, superhydrophobic paints were created by subsequent hydrophobilization. The HCNT–SNP composite coatings were finally fabricated by spray-coated methods onto various substrates in one step. The detailed procedure is described in ESI (Materials and methods†). The microscopic morphologies of the samples were characterized by transmission electron microscopy (TEM) and field-emission scanning electron microscopy (FESEM). Optical photographs of dewdrop dynamics were captured by a high speed camera. As expected, continuous CDSE behaviors were indeed shown on the sprayable HCNT–SNP composite coating.

In Fig. 1, we demonstrate the self-assembly process of HCNT–SNP composite nano-tubes. TEM images suggest that SNPs could be successfully assembled on a smooth HCNT (Fig. 1a) wall to obtain a rough composite nano-tube (Fig. 1b) under base catalysis conditions. After spray painting, a nano-porous foam-like coating was obtained by random multilayer stacking of the soft and rough nano-tubes (Fig. 1c). The superhydrophobicity of the composite coating was evaluated by a contact angle meter, which achieves static water contact angles (SCAs) of over 160° and roll-off angles (RAs) of under 5° (Fig. S1, ESI†). To further exhibit the wettability, a water droplet bouncing test (Fig. 1c) was carried out with 5 μL droplet perpendicular impacts from 3 cm high. The droplet completely left the coating without wetting, contaminating, penetrating or damaging the coating, and the contact time (Δt_c) between the droplet and the coating from encounter to separation is about 9.0 ms. Simultaneously, we also fabricated fluorinated HCNT (F-HCNT) paint by directly modifying the HCNT in alkaline solution without tetraethyl orthosilicate. As shown in Fig. S2 (ESI†), the F-HCNT coating presents the same superhydrophobicity
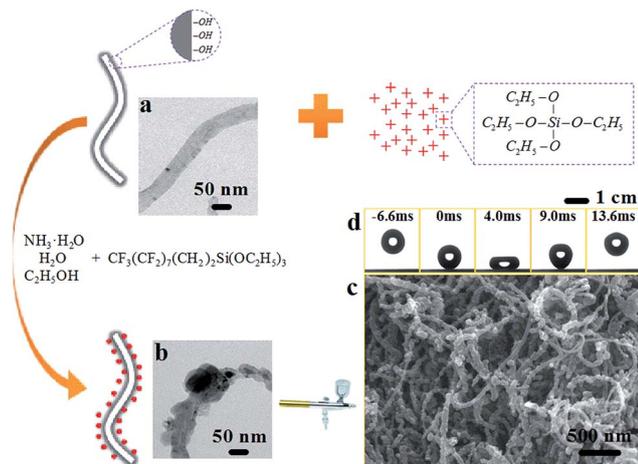
Fig. 1 Schematic diagrams of synthesizing superhydrophobic HCNT–SNP composite nano-tube. TEM images of (a) HCNT and (b) HCNT–SNP composite nano-tube. (c) FESEM image and (d) water droplet bouncing test of HCNT–SNP composite coating by one-step spray.

when measured by macroscopic water droplets (SCA > 160°, RA < 5° and $\Delta t_c \sim 9.0$ ms). However, according to previous studies,[33] abundant nano-porosities from random multilayer stacking of rough hydrophobic nano-chains are the key to realizing CDSE due to their ensuring an extremely low solid–liquid interface adhesion and avoiding the penetration of moisture. Thus, we could predict that the dewdrops could just slip under the effect of gravity because of the lack of nano-pore coatings stacked by F-HCNT (Fig. S3, ESI†).

Condensation tests were carried out on a vertical cooling stage with the conditions of a substrate temperature of 2 °C, ambient temperature of 15 °C, relative humidity of 70%, and dew-point temperature of 9.58 °C. Here, to investigate the condensation performance on superhydrophobic HCNT–SNP and F-HCNT coatings, we sprayed the above two paints on polished stainless steel sheets with a size of 50 × 50 mm. Fig. 2a shows the coalescence and departure behaviors of four adjacent

dewdrops with sizes of ~50 μm without any external force (Video S1, ESI†). To understand the dynamics of the jumping drop, we also investigated the movement track of dewdrops. Fig. 2b suggests that the dewdrop departed with a speed of about ~5 m s^{-1} from the coating (Video S1, ESI†). It has been reported that the initial kinetic energy of the jumping drop is provided by the residual energy from the released surface energy after overcoming viscous flow-induced energy dissipation and interfacial adhesion-induced energy dissipation.[34] Here, we assumed that all the droplet radii (R_0) are equal before coalescence. Accordingly, the $R = N^{1/3}R_0$ is the droplet radius after coalescence, where N is the total number of droplets (N) participating in the jumping behavior. As shown previously,[35] the initial jumping speed (U) could be roughly calculated from the following formula (1).

$$U = \sqrt{\frac{6\gamma_{LV}}{\rho R}\left(N^{1/3} - 1\right)}, \quad (N \geq 2) \tag{1}$$

where, $\gamma_{LV} = 0.075$ N m^{-1} is the surface tension of water, $\rho = 1.0 \times 10^3$ kg m^{-3} is the water density. Fig. 2c shows that the initial jumping velocities are fixed at 1.97–7.21 m s^{-1} when the value ranges of the droplet radii and numbers are 10–30 μm and 2–10.

Based on the CDSE function on the HCNT–SNP coating, we also examined the statistical parameters of dewdrops on a horizontal cooling stage under the above condensation conditions. Fig. 3a shows that spherical condensed micro-drops were demonstrated on the HCNT–SNP coating. After 20 min, their sizes maintain a relatively dynamic balance, containing a few of intermediate size and a new generation of dew droplets. Fig. S4 (ESI†) captures that two or more adjacent water droplets with a Cassie–Baxter state bounced off their initial position without any external force. As expected, the dynamic characteristics of dewdrops on the F-HCNT coating differ markedly from those on the HCNT–SNP surface. Continuous merging and growth processes were surveyed on the F-HCNT coating and large dewdrops (over 100 μm) could be found everywhere after 20 min (Fig. 3b).
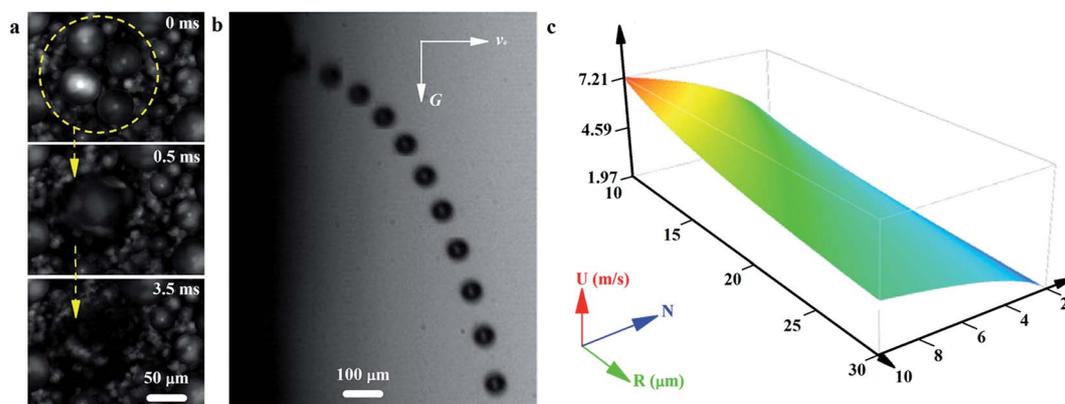

Fig. 2 Typical CDSE behaviors on the HCNT–SNP composite coating placed vertically. (a) Time lapse images of dewdrops captured via a high speed camera, showing the self-jumping behavior of four drops with a size of ~50 μm from the top-view. (b) The self-jumping movement track of a dewdrop with a diameter of ~50 μm demonstrated by an overlapped optical image from the side-view. (c) Relationship among the initial jumping speed (U), droplet radius (R) after merging and the total number of droplets (N) before merging.
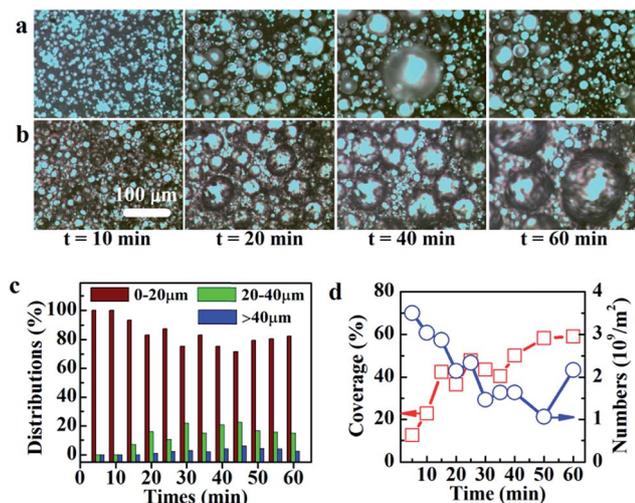
Fig. 3 Dynamic optical micrographs of condensed droplets on (a) HCNT–SNP and (b) F-HCNT superhydrophobic coating. (c) Number distributions of dewdrops against time since condensation on HCNT–SNP coating. (d) The coverage of condensed dewdrops and number of units changed with time on HCNT–SNP coating.

Fig. 3c and d show how the size distribution, coverage, and numbers of dewdrops on HCNT–SNP surfaces change with time. The nucleation and growth of the condensed droplets were mainly developed at 0–10 min. At 10 min, the dimensions of the droplets are below 20 μm with a low coverage rate (under 25%) and a high nucleation rate (over $3 \times 10^9\ \mathrm{m}^{-2}$). Under these circumstances, the CDSE behaviors were only detected in a tiny region. As a consequence, the statistical parameters of dewdrops are similar between the HCNT–SNP and F-HCNT surfaces. At 20 min, over 15% of drops have grown to 20–40 μm on the HCNT–SNP coating. After that, the size distribution of the drops with a size of 0–20 μm could be maintained in a limited range (70–90%).

In conclusion, we fabricated a sprayable superhydrophobic HCNT–SNP composite coating with a CDSE function by a self-assembly process and subsequent chemical modification. This work offers a new insight into developing the function of CNT in self-cleaning and anti-condensation by one-step spray coating on various substrates. The results of condensation testing have shown that CDSE behaviors could be widely captured on the HCNT–SNP composite coating. About 80% of dewdrops hold their sizes below 20 μm after 60 min, which shows that these coatings promise to be good candidates for improving the condensation heat transfer of heat exchangers in the future.

Acknowledgements

References

1 R. L. Bond, R. Holland, G. W. Smith and G. G. Thurlow, Coal Extracts as Promoters of Dropwise Condensation of Steam, *Nature*, 1956, **178**, 431.

2 C.-H. Chen, Q. Cai, C. Tsai, C.-L. Chen, G. Xiong, Y. Yu and Z. Ren, Dropwise condensation on superhydrophobic surfaces with two-tier roughness, *Appl. Phys. Lett.*, 2007, **90**, 173108.

3 N. Miljkovic, R. Enright, Y. Nam, K. Lopez, N. Dou, J. Sack and E. N. Wang, Jumping-droplet-enhanced condensation on scalable superhydrophobic nanostructured surfaces, *Nano Lett.*, 2013, **13**, 179–187.

4 X. Chen, R. Ma, H. Zhou, X. Zhou, L. Che, S. Yao and Z. Wang, Activating the microscale edge effect in a hierarchical surface for frosting suppression and defrosting promotion, *Sci. Rep.*, 2013, **3**, 2515.

5 J. Zhu, Y. Luo, J. Tian, J. Li and X. Gao, Clustered ribbed-nanoneedle structured copper surfaces with high-efficiency dropwise condensation heat transfer performance, *ACS Appl. Mater. Interfaces*, 2015, **7**, 10660–10665.

6 K. Rykaczewski, J. Chinn, M. L. Walker, J. H. J. Scott, A. Chinn and W. Jones, Dynamics of Nanoparticle Self-Assembly into Superhydrophobic Liquid Marbles during Water Condensation, *ACS Nano*, 2011, **5**, 9746–9754.

7 R. Enright, N. Miljkovic, A. Al-Obeidi, C. V. Thompson and E. N. Wang, Condensation on superhydrophobic surfaces: the role of local energy barriers and structure length scale, *Langmuir*, 2012, **28**, 14424–14432.

8 H. Jo, K. W. Hwang, D. Kim, M. Kiyofumi, H. S. Park, M. H. Kim and H. S. Ahn, Loss of superhydrophobicity of hydrophobic micro/nano structures during condensation, *Sci. Rep.*, 2015, **5**, 9901.

9 J. Li, Y. Luo, J. Zhu, H. Li and X. Gao, Subcooled-Water Nonstickiness of Condensate Microdrop Self-Propelling Nanosurfaces, *ACS Appl. Mater. Interfaces*, 2015, **7**, 26391–26395.

10 J. Li, W. Zhang, Y. Luo, J. Zhu and X. Gao, Facile Fabrication of Anodic Alumina Rod-Capped Nanopore Films with Condensate Microdrop Self-Propelling Function, *ACS Appl. Mater. Interfaces*, 2015, **7**, 18206–18210.

11 Q. Xu, J. Li, J. Tian, J. Zhu and X. Gao, Energy-effective frost-free coatings based on superhydrophobic aligned nanocones, *ACS Appl. Mater. Interfaces*, 2014, **6**, 8976–8980.

12 Y. Zhao, Y. Luo, J. Li, F. Yin, J. Zhu and X. Gao, Condensate microdrop self-propelling aluminum surfaces based on controllable fabrication of alumina rod-capped nanopores, *ACS Appl. Mater. Interfaces*, 2015, **7**, 11079–11082.

13 Y. Zhao, Y. Luo, J. Zhu, J. Li and X. Gao, Copper-Based Ultrathin Nickel Nanocone Films with High-Efficiency Dropwise Condensation Heat Transfer Performance, *ACS Appl. Mater. Interfaces*, 2015, **7**, 11719–11723.

14 H. Li, J. Zhu, Y. Luo, F. Yu, J. Fang and X. Gao, Situ Growth of Densely Packed Single-Crystal Copper Nanocone Structure Films with Condensate Microdrop Self-Removal Function on Copper Surfaces, *Adv. Mater. Interfaces*, 2016, **3**, 1600362.

15 W. Zhang, G. Lin, J. Li, H. Xue, Y. Luo and X. Gao, Fabrication of Biomimetic Polymer Nanocone Films with Condensate Microdrop Self-Removal Function, *Adv. Mater. Interfaces*, 2015, **2**, 1500238.

16 Y. Luo, J. Li, J. Zhu, Y. Zhao and X. Gao, Fabrication of condensate microdrop self-propelling porous films of cerium oxide nanoparticles on copper surfaces, *Angew. Chem., Int. Ed.*, 2015, **54**, 4876–4879.

17 Y. Luo, X. Gong, Y. Chen, J. Zhu, J. Wei and X. Gao, Design and Fabrication of a Tip-Like ZnO Nanotube Array Structure with Condensate Microdrop Self-Propelling Function, *ChemNanoMat*, 2016, **2**, 1018–1022.

18 J. B. Boreyko and C.-H. Chen, Self-Propelled Dropwise Condensate on Superhydrophobic Surfaces, *Phys. Rev. Lett.*, 2009, **103**, 184501.

19 C. Lv, P. Hao, Z. Yao and F. Niu, Departure of condensation droplets on superhydrophobic surfaces, *Langmuir*, 2015, **31**, 2414–2420.

20 J. Y. Huang, Y. K. Lai, F. Pan, L. Yang, H. Wang, K. Q. Zhang, H. Fuchs and L. F. Chi, Multifunctional superamphiphobic TiO2 nanostructure surfaces with facile wettability and adhesion engineering, *Small*, 2014, **10**, 4865–4873.

21 J. Li, R. Wu, Z. Jing, L. Yan, F. Zha and Z. Lei, One-step spray-coating process for the fabrication of colorful superhydrophobic coatings with excellent corrosion resistance, *Langmuir*, 2015, **31**, 10702–10707.

22 Y. Zhang, D. Ge and S. Yang, Spray-coating of superhydrophobic aluminum alloys with enhanced mechanical robustness, *J. Colloid Interface Sci.*, 2014, **423**, 101–107.

23 X. Tian, S. Shaw, K. R. Lind and L. Cademartiri, Thermal Processing of Silicones for Green, Scalable, and Healable Superhydrophobic Coatings, *Adv. Mater.*, 2016, **28**, 3677–3682.

24 Y. Lu, S. Sathasivam, J. Song, C. R. Crick, C. J. Carmalt and I. P. Parkin, Robust self-cleaning surfaces that function when exposed to either air or oil, *Science*, 2015, **347**, 1132–1135.

25 Z. Zhang, B. Ge, X. Men and Y. Li, Mechanically durable, superhydrophobic coatings prepared by dual-layer method for anti-corrosion and self-cleaning, *Colloids Surf., A*, 2016, **490**, 182–188.

26 X. Zhang, Y. Si, J. Mo and Z. Guo, Robust micro-nanoscale flowerlike ZnO/epoxy resin superhydrophobic coating with rapid healing ability, *Chem. Eng. J.*, 2017, **313**, 1152–1159.

27 J. T. Han, S. Y. Kim, J. S. Woo and G.-W. Lee, Transparent, Conductive, and Superhydrophobic Films from Stabilized Carbon Nanotube/Silane Sol Mixture Solution, *Adv. Mater.*, 2008, **20**, 3724–3727.

28 I. S. Bayer, A. Steele and E. Loth, Superhydrophobic and electroconductive carbon nanotube-fluorinated acrylic copolymer nanocomposites from emulsions, *Chem. Eng. J.*, 2013, **221**, 522–530.

29 R. Enright, N. Miljkovic, J. Sprittles, K. Nolan, R. Mitchell and E. N. Wang, How Coalescing Droplets Jump, *ACS Nano*, 2014, **8**, 10352–10362.

30 X. Chen, J. Wu, R. Ma, M. Hua, N. Koratkar, S. Yao and Z. Wang, Nanograssed Micropyramidal Architectures for Continuous Dropwise Condensation, *Adv. Funct. Mater.*, 2011, **21**, 4617–4623.

31 C. Lv, P. Hao, X. Zhang and F. He, Dewetting Transitions of Dropwise Condensation on Nanotexture-Enhanced Superhydrophobic Surfaces, *ACS Nano*, 2015, **9**, 12311–12319.

32 J. Liu, H. Guo, B. Zhang, S. Qiao, M. Shao, X. Zhang, X. Q. Feng, Q. Li, Y. Song, L. Jiang and J. Wang, Guided Self-Propelled Leaping of Droplets on a Micro-Anisotropic Superhydrophobic Surface, *Angew. Chem., Int. Ed.*, 2016, **55**, 4265–4269.

33 S. Wang, W. Zhang, X. Yu, C. Liang and Y. Zhang, Sprayable superhydrophobic nano-chains coating with continuous self-jumping of dew and melting frost, *Sci. Rep.*, 2017, **7**, 40300.

34 J. Tian, J. Zhu, H.-Y. Guo, J. Li, X.-Q. Feng and X. Gao, Efficient Self-Propelling of Small-Scale Condensed Microdrops by Closely Packed ZnO Nanoneedles, *J. Phys. Chem. Lett.*, 2014, **5**, 2084–2088.

35 M. K. Kim, H. Cha, P. Birbarah, S. Chavan, C. Zhong, Y. Xu and N. Miljkovic, Enhanced Jumping Droplet Departure, *Langmuir*, 2015, **31**, 13452–13466.